DNA Double-Strand Break Repair of Blood Lymphocytes and Normal Tissues Analysed in a Preclinical Mouse Model: Implications for Radiosensitivity Testing

Claudia E. Rübe,[1] Saskia Grudzenski,[2] Martin Kühne,[1] Xiaorong Dong,[1,3] Nicole Rief,[2] Markus Löbrich,[2] and Christian Rübe[1]

Abstract

Purpose: Radiotherapy is an effective cancer treatment, but a few patients suffer severe radiation toxicities in neighboring normal tissues. There is increasing evidence that the variable susceptibility to radiation toxicities is caused by the individual genetic predisposition, by subtle mutations, or polymorphisms in genes involved in cellular responses to ionizing radiation. Double-strand breaks (DSB) are the most deleterious form of radiation-induced DNA damage, and DSB repair deficiencies lead to pronounced radiosensitivity. Using a preclinical mouse model, the highly sensitive γH2AX-foci approach was tested to verify even subtle, genetically determined DSB repair deficiencies known to be associated with increased normal tissue radiosensitivity.

Experimental Design: By enumerating γH2AX-foci in blood lymphocytes and normal tissues (brain, lung, heart, and intestine), the induction and repair of DSBs after irradiation with therapeutic doses (0.1-2 Gy) was investigated in repair-proficient and repair-deficient mouse strains *in vivo* and blood samples irradiated *ex vivo*.

Results: γH2AX-foci analysis allowed to verify the different DSB repair deficiencies; even slight impairments caused by single polymorphisms were detected similarly in both blood lymphocytes and solid tissues, indicating that DSB repair measured in lymphocytes is valid for different and complex organs. Moreover, γH2AX-foci analysis of blood samples irradiated *ex vivo* was found to reflect repair kinetics measured *in vivo* and, thus, give reliable information about the individual DSB repair capacity.

Conclusions: γH2AX analysis of blood and tissue samples allows to detect even minor genetically defined DSB repair deficiencies, affecting normal tissue radiosensitivity. Future studies will have to evaluate the clinical potential to identify patients more susceptible to radiation toxicities before radiotherapy.

Radiotherapy is an effective cancer treatment, but, even with highly conformal treatment planning, associated radiation toxicities in neighboring normal tissues remain the major limiting factor for delivering tumoricidal doses. Clear differences exist between patients regarding their individual normal tissue responses after radiotherapy. Even after strictly identical treatment modalities, some patients seem to tolerate the treatment well, whereas others develop severe radiation-induced side effects. There is increasing evidence that the patient-to-patient variability in normal tissue response is caused primarily by their genetic predisposition, by subtle mutations, or polymorphisms in genes involved in cellular responses to radiation (1–3). Predictive assays that accurately determine normal tissue tolerance in individual patients would permit to modify the treatment in radiosensitive individuals to prevent severe side effects and to intensify radiotherapy in relatively resistant patients, thereby improving the therapeutic ratio in cancer treatment (4–6).

DNA double-strand breaks (DSB) are the most deleterious form of radiation-induced DNA damage, and numerous *in vitro* studies emphasize the tremendous effect of efficient DSB response systems on cell survival after exposure to ionizing radiation (7–10). Furthermore, heritable genetic disorders, such as Ataxia-telangiectasia (A-T) and LIG-4 syndromes, characterized by well-defined deficiencies in DSB repair, are associated with pronounced clinical radiosensitivity (11–16). Such highly expressing familial genetic disorders are rare, but other minor deficiencies based on polymorphisms in DNA

Authors' Affiliations: [1]Department of Radiation Oncology, Saarland University, Homburg/Saar, Germany; [2]Radiation Biology and DNA Repair, Darmstadt University of Technology, Darmstadt, Germany; and [3]Cancer Center, Union Hospital Tongji Medical College, Huazhong University of Science and Technology, Wuhan, P.R. China

Received 12/17/07; revised 6/5/08; accepted 6/22/08.

Grant support: Saarland University grant HOMFOR 2006/77 (C.E. Rübe) and in part by the Bundesministerium für Bildung und Forschung through the Forschungszentrum Karlsruhe grant 02S8132 (M. Löbrich).

The costs of publication of this article were defrayed in part by the payment of page charges. This article must therefore be hereby marked *advertisement* in accordance with 18 U.S.C. Section 1734 solely to indicate this fact.

Requests for reprints: Claudia E. Rübe, Department of Radiation Oncology, Saarland University, 66421 Homburg/Saar, Germany. Phone: 49-6841-1624884; Fax: 49-6841-1621401; E-mail: claudia.ruebe@uniklinik-saarland.de or Markus Löbrich, Radiation Biology and DNA Repair, Darmstadt University of Technology, 64287 Darmstadt, Germany. E-mail: Lobrich@bio.tu-darmstadt.de.

doi:10.1158/1078-0432.CCR-07-5147

Translational Relevance

About 50% of patients with malignant tumors receive radiotherapy with curative or palliative intent. Most patients seem to tolerate radiotherapy well, but a few patients suffer severe radiation-induced side effects, even after strictly identical treatment. New insights suggest that the increased susceptibility to radiation toxicities may result from subtle mutations or polymorphisms in DNA damage – response genes. The most deleterious form of radiation-induced DNA damage are double-strand breaks (DSB), and deficiencies in repairing DSBs cause pronounced radiosensitivity. Using a preclinical mouse model, we tested the highly sensitive γH2AX-foci analysis to verify even subtle, genetically determined DSB repair deficiencies known to be associated with increased normal tissue radiosensitivity. Most notably, γH2AX-foci analysis of blood lymphocytes provides precise information about the genetically defined DSB repair capacity, shown to be valid for different and complex organs in a given individual. Because DSB repair capacity is a determining factor for normal tissue responses not only after ionizing radiation, but also after treatment with DNA-damaging chemotherapeutics, the γH2AX-foci analysis of blood samples, applicable in diagnostic routine, can possibly serve as general predictive test in cancer treatment to identify patients more susceptible to normal tissue toxicities.

damage response genes are expected to be more common in the human population.

Despite significant advances in the mechanistic understanding of DSB repair pathways, only little is known about the induction and processing of radiation-induced DSBs *in vivo*, i.e., in complex cell systems of normal tissues under physiological conditions of living organisms. The analysis of DSB repair has, for many years, relied on techniques such as pulsed-field gel electrophoresis that require high irradiation doses and, thus, was restricted to *in vitro* studies. Recently, the γH2AX-foci approach, an extraordinarily sensitive technique to monitor DSB repair even after therapeutic and diagnostic irradiation doses, has been established (17, 18). After ionizing irradiation, histone H2AX molecules in megabase chromatin regions adjacent to break sites are phosphorylated within minutes on serine-139 residues. This phosphorylated form of H2AX, termed γH2AX, can be visualized by immunofluorescence analysis and forms discrete nuclear foci, which reflect sites of DSBs. γH2AX-foci analysis is a highly sensitive technique to detect DSBs, and the kinetics of γH2AX-foci loss strongly correlate with the time course of DSB repair (19, 20).

In the present study, we tested the γH2AX-foci approach for its potential to verify even subtle, genetically determined DSB repair deficiencies known to be associated with increased clinical radiosensitivity. For this purpose, we investigated the repair of DSBs in various mouse strains, which harbor defined DSB repair deficiencies. Highly radiosensitive severe combined immunodeficiency (SCID) mice have a major DSB repair defect caused by a spontaneous mutation in the gene encoding the catalytic subunit of the DNA-dependent protein kinase (DNA-PKcs; ref. 21). DNA-PKcs is a core protein of nonhomologous DNA end-joining (NHEJ), generally considered the predominant pathway for repairing DSBs in mammalian cells (22, 23). BALB/c mice possess two naturally occurring single nucleotide polymorphisms in the DNA-PKcs gene, which reduce but do not eliminate DNA-PKcs activity (24). Among commonly used inbred mouse strains, BALB/c mice have been consistently found to be unusually radiosensitive (24, 25). A-T mice harbor mutations in the A-T – mutated (ATM) protein and are also characterized by increased radiosensitivity and a predisposition to cancer (26 – 29). A-T – mutated protein is the central component of the signal transduction pathway responding to DSBs and regulates a component of DSB repair by NHEJ (14 – 16, 30 – 32). Here, we established the γH2AX-foci approach in blood lymphocytes and various normal tissues to investigate the repair of DSBs in SCID, BALB/c, and A-T mice compared with repair-proficient C57BL/6 mice.

Using this preclinical mouse model, we evaluate the feasibility of the γH2AX-foci approach to verify DSB repair deficiencies as a valuable tool in predictive testing for clinical normal tissue radiosensitivity.

Materials and Methods

***Animal irradiation* (in vivo).** Adult SCID (CB17/Icr-Prkdc scid/Crl), A-T (129S6/SvEvTac-Atm-tm1Awb-/J), BALB/c (BALB/cAnNCrl), and C57BL/6 (C57BL/6NCrl) mice (Charles River Laboratories) received whole body irradiation with 0.1, 0.5, 1, or 2 Gy, respectively (linear accelerator, 6MV-photons; dose-rate, 2 Gy/min). The experimental protocol was approved by the Medical Sciences Animal Care and Use Committee of the University of Saarland.

Blood/tissue isolation. For DSB induction in different tissues, 3 C57BL/6 mice per dose were analyzed 10 min postirradiation. For DSB repair kinetics, 3 different mice per strain were analyzed at 0.5, 2.5, 5, 24, and 48 h postirradiation. In each case, three sham-irradiated mice per strain served as controls. After anesthesia, blood was harvested by aortal puncture; subsequently, brain, lung, heart, small intestine were immediately removed and placed in fixative. Formalin-fixed tissues were embedded in paraffin and sectioned at a thickness of 4 μm.

***Blood irradiation* (ex vivo).** Whole blood of BALB/c and C57BL/6 mice were irradiated *ex vivo* (X-ray, 90 kV and 19 mA; dose-rate, 2 Gy/min), and DSB repair kinetics were evaluated in isolated lymphocytes at 0.5, 2.5, 5, and 8 h postirradiation (3 mice per strain per time point, 3 sham-irradiated controls per strain). For DSB induction (5 min postirradiation), isolated lymphocytes were irradiated *ex vivo* to prevent repair during isolation process.

γH2AX-immunofluorescence (blood lymphocytes). Lymphocyte separation was done according to the manufacturer's instructions (Percoll; PAA). Isolated lymphocytes were fixed in formaldehyde, washed in Tween 20 and spotted onto coverslips. Samples were fixed in methanol, permeabelized in acetone, and incubated with anti-γH2AX antibody (Upstate; 1:800) followed by Alexa Fluor 488 – conjugated goat-anti-mouse secondary antibody (Invitrogen; 1:400). Afterwards, samples were mounted in VECTAshield with 4′,6-diamidino-2-phenylindole (Vector Laboratories).

γH2AX-immunohistochemistry (tissues). After dewaxing in xylene and rehydration in graded alcohols, tissue sections were boiled in citrate buffer, preincubated with H_2O_2, and blocked with rabbit serum (PAA). Afterwards, sections were incubated with anti-γH2AX antibody (Upstate; 1:800 dilution), followed by biotinylated goat-anti-rabbit antibody (Dako; 1:200). Sections were labeled by avidin-biotin-peroxidase complex, followed by diaminobenzidine development (Sigma-Aldrich). Finally, sections were counterstained with hematoxylin and mounted in Entellan (Merck).

γH2AX-immunofluorescence (tissues). After dewaxing in xylene and rehydration in graded alcohols, sections were boiled in citrate buffer

and preincubated with goat serum (ICN). Afterwards sections were incubated with anti-γH2AX antibody (Upstate; 1:800), followed by Alexa Fluor 488–conjugated goat-anti-mouse secondary antibody (Invitrogen; 1:200). Finally, sections were mounted in VECTAshield with 4′,6-diamidino-2-phenylindole (Vector Laboratories).

Colocalization of γH2AX and 53BP1 (tissues). For double labeling, sections were incubated with anti-γH2AX antibody (Upstate; 1:400) and anti-53BP1 (Bethyl; 1:200) followed by Alexa Fluor 488– and Rhodamine-Red–conjugated secondary antibodies (Invitrogen; 1:400).

Foci analysis. Fluorescence images were captured by using Nikon E600-epifluorescent microscope equipped with charge-coupled device camera and acquisition software (Nikon). For quantitative analysis, foci were counted by eye using objective magnification of ×60 and ×100. Foci counting was done until at least 40 cells and 40 foci (lymphocytes) or 80 cells and 40 foci (tissues) were registered for each data point.

Statistical analysis. To evaluate potential differences in the DSB repair capacity of the various mouse strains (SCID, A-T, BALB/c, and C57BL/6), the statistical comparisons were done at each time point (0.5, 2.5, 5, 24, and 48 h postirradiation) by ANOVA Bonferroni Post hoc test, using the statistical software SPSS Version 15 (SPSS, Inc.). The criterion for statistical significance was a P value of <0.05.

Results

***DSB repair in blood lymphocytes* (in vivo).** First, we analyzed the DSB repair *in vivo* by counting γH2AX-foci in blood lymphocytes after whole-body irradiation of the mice. Representative examples of γH2AX-labeled blood lymphocytes analyzed at 0.5, 2.5, 5, and 24 hours after irradiation with 2 Gy are depicted in Fig. 1A. The time course of γH2AX-foci loss in blood lymphocytes of the different mouse strains after exposure to 2Gy is shown in Fig. 1B. Although similar numbers of γH2AX-foci were observed at 5 minutes postirradiation (Fig. 1B, *inset*; ~23 foci per cell), the various mouse strains showed clearly distinct kinetics of foci loss. Lymphocytes from repair-proficient C57BL/6 mice exhibited a rapid decrease in foci number within the first hours (0.5-5 hours) postirradiation. This fast component of foci loss was followed by a slower process at later times, and only very low levels of damage were observed at 24 hours (1.0 foci per cell) and 48 hours (0.5 foci per cell) postirradiation. As expected, DNA-PKcs–deficient lymphocytes of SCID mice known to be severely deficient in DSB rejoining showed considerably increased γH2AX-foci numbers at all analyzed repair times ($P < 0.0001$), consistent with the involvement of DNA-PKcs in the fast and slow component of DSB repair. We also investigated A-T mice deficient for A-T mutated, whose specific involvement in the slow component of DSB repair was recently established with fibroblast cell cultures (30). Significantly, A-T mice showed elevated levels of remaining foci at later time points (5-48 hours) postirradiation ($P < 0.006$), but foci numbers similar to C57BL/6 mice after short repair times (0.5-2.5 hours). Thus, both SCID and A-T mice with distinct deficiencies in DSB repair show kinetics of γH2AX-foci loss, which closely mirror the DSB repair defects of DNA-PKcs– and A-T–mutated-deficient cell systems *in vitro* (14, 22). We also tested BALB/c mice with described radiosensitivity that seems to result from a polymorphism in DNA-PKcs (24, 25). Compared with radioresistant C57BL/6 mice, blood lymphocytes derived from radiosensitive BALB/c mice revealed slightly increased foci levels at 5 and 24 hours ($P < 0.043$) but not at 48 hours postirradiation. This phenotype is consistent with a slightly slower but functional DSB repair process in BALB/c mice. Collectively, our data show that analyzing the kinetics for γH2AX-foci loss can be used to assess the DSB repair capacity in lymphocytes of irradiated mice.

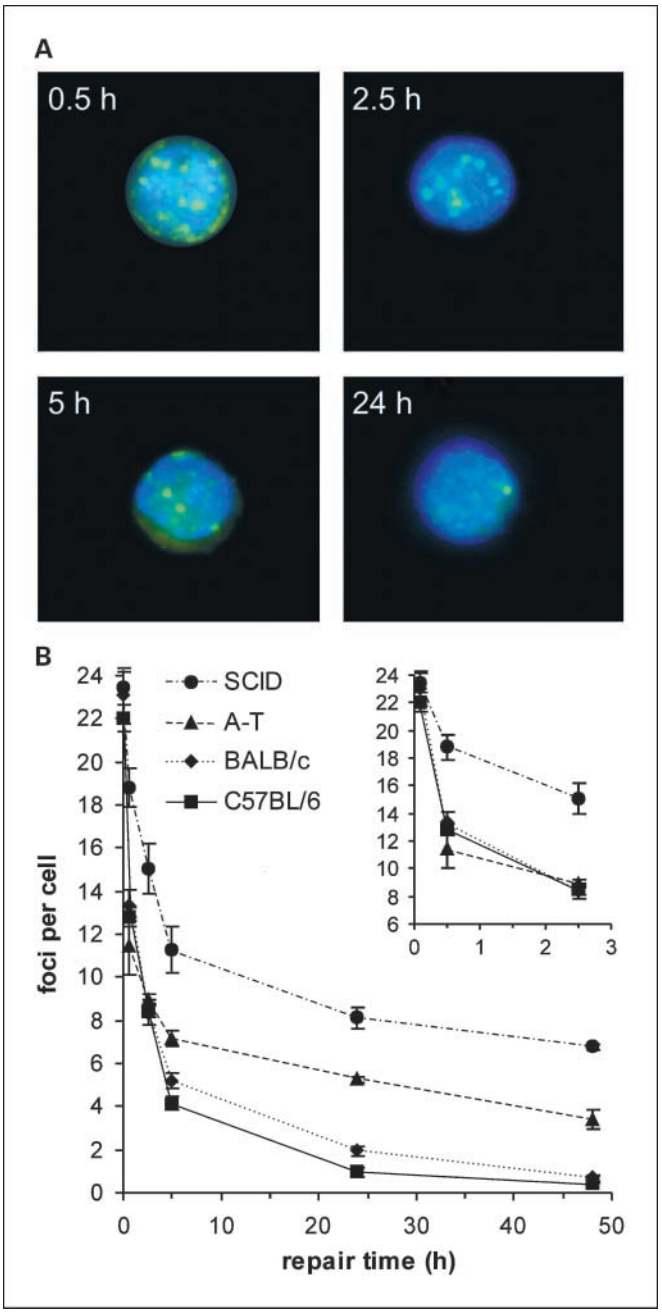

Fig. 1. *A,* γH2AX-immunofluorescence staining in blood lymphocytes analyzed at 0.5, 2.5, 5, and 24 h after *in vivo* irradiation (2 Gy) of repair-proficient C57BL/6 mice. Note that the images show optical sections providing information from only a thin focal plane. For enumerating γH2AX-foci per cell, the whole depth of the nuclei was scanned by focusing manually along the optical axis (z-direction; original magnification, ×1,000) *B,* γH2AX-foci analysis in blood lymphocytes of repair-deficient (SCID, A-T, BALB/c) and repair-proficient (C57BL/6) mouse strains after *in vivo* irradiation (2 Gy). Scoring the loss of γH2AX-foci allowed us to verify the different, genetically determined DSB repair deficiencies, including the minor impairment of BALB/c mice. Points, mean from three experiments; bars, SE.

γH2AX-immunohistochemistry and γH2AX-immunofluorescence in tissues. To investigate to what extent DSB repair measured in peripheral blood lymphocytes correlates with the DSB repair of complex solid tissues, we established

γH2AX-immunohistochemistry and γH2AX-immunofluorescence. Combining these two staining techniques permits both accurate identification of cells in complex tissue morphology and precise quantification of γH2AX-foci numbers per cell.

Figure 2A shows the immunohistochemical staining of γH2AX in brain, lung, heart, and small intestine of repair-proficient C57BL/6 mice analyzed at 0.5 hours post-2 Gy irradiation compared with unirradiated controls. After testing different antigen retrievals and optimizing staining procedures, nearly 100% of the nuclei in brain, lung, heart, and small intestine stained positively for γH2AX at 0.5 hours after irradiation with 2 Gy, whereas unirradiated tissues were almost completely negative for γH2AX. Although the nuclear γH2AX-staining intensity increased with irradiation dose and decreased with postirradiation repair time, γH2AX-immunohistochemistry does not provide a real quantitative assessment but allows the allocation of DSBs to the nuclei of the different cell types in complex tissues.

Please note that the pictures of unirradiated tissue samples in Fig. 2A were consciously chosen to show some kind of positive staining, demonstrating that all tissue sections were stained in the same way. Although in the unirradiated brain tissue, the diffuse γH2AX staining of the single nucleus presumably belongs to an apoptotic cell (33–35), the discrete punctuate γH2AX staining, visible in only very few cells of unirradiated tissues, likely reflects naturally occurring DSBs arising from biological or environmental sources, best perceptible in unirradiated heart tissue (Fig. 2A, *arrows*).

Figure 2B shows representative examples of γH2AX-immunofluorescence staining in the different tissues at 0.5 and 5 hours after irradiation with 2 Gy compared with unirradiated controls. Although unirradiated normal tissues were predominantly negative for γH2AX-foci, discrete nuclear γH2AX-foci were observed at 0.5 and 5 hours postirradiation. The clear reduction in foci number with time (apparent between 0.5 and 5 hours in all analyzed tissues, compare Fig. 2B) indicates that γH2AX-immunofluorescence analysis can be used to quantify DSBs in solid tissues and, thus, provides the opportunity to measure DSB repair in complex organs.

It is noteworthy that the diffuse background staining is caused by the standardized fixation process used to precipitate the protein components to preserve the structural integrity of the tissue samples. This aldehyde fixation creates tissue-specific autofluorescence by forming cross-linkages between cellular

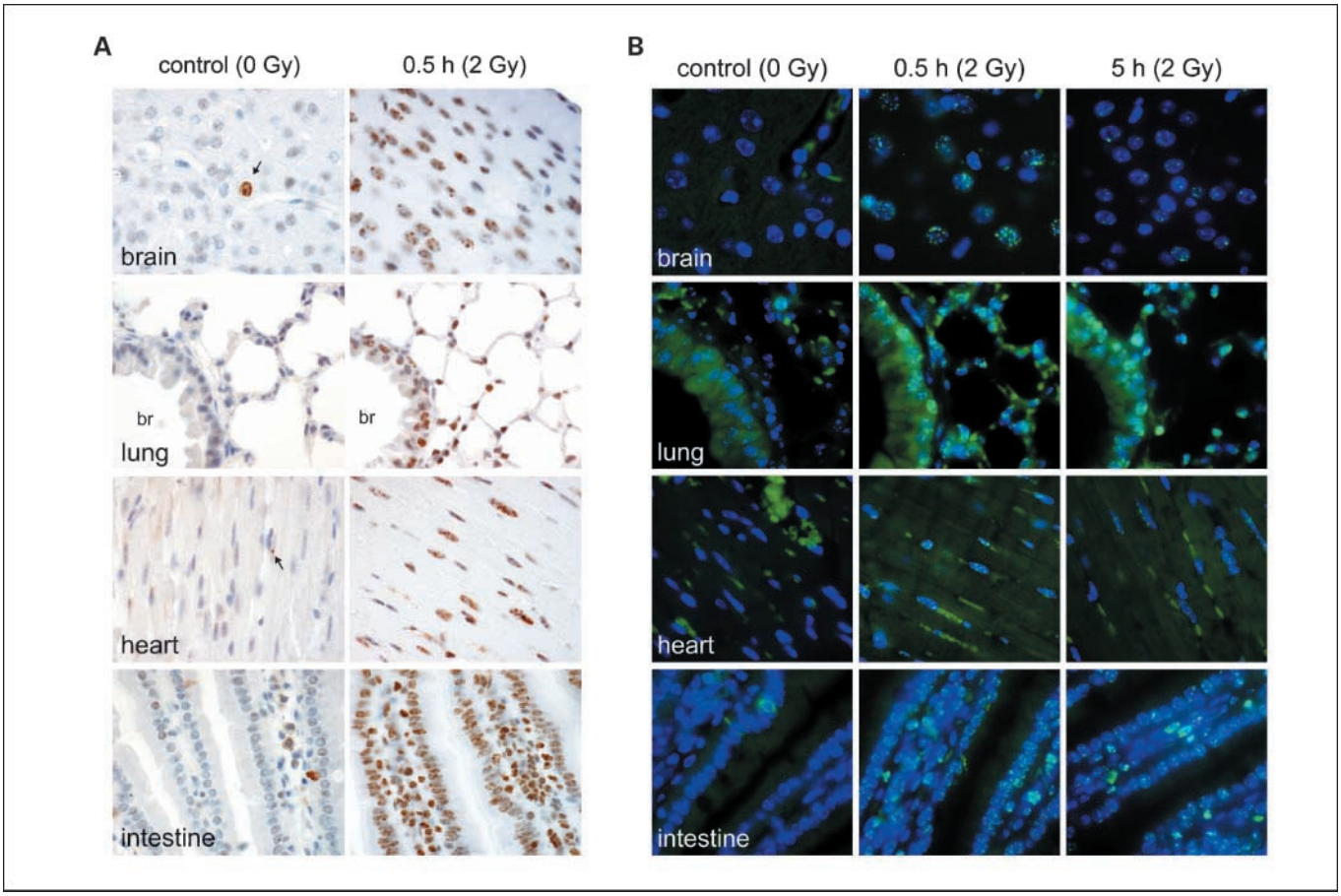

Fig. 2. *A,* immunohistochemical staining of γH2AX (diaminobenzidine, *brown*) in brain, lung, heart, and small intestine at 0.5 h after *in vivo* irradiation (2 Gy) compared with unirradiated controls. Unirradiated normal tissues were almost completely negative for γH2AX, except for the diffuse γH2AX-stained nucleus belonging presumably to an apoptotic cell (unirradiated brain), and very sparsely distributed punctuate γH2AX-staining likely reflecting naturally occurring DSBs, best perceptible in unirradiated heart tissue (*arrows*). In contrast, an intense granular staining of nearly all nuclei was apparent after irradiation (*br,* bronchiolar epithelium; original magnification, ×600). *B,* immunofluorescence staining of γH2AX (FITC, *green*) in brain, lung, heart, and small intestine at 0.5 and 5 h after *in vivo* irradiation (2 Gy) compared with unirradiated control. Although unirradiated tissues were predominantly negative, discrete nuclear γH2AX-foci were observed at 0.5 and 5h postirradiation. The time-dependent reduction in foci number indicates that γH2AX-immunofluorescence can be used to measure DSB repair. Note that the images show just cross-sections; for enumerating γH2AX-foci, a manual z-scan covering the entire nucleus in the three-dimensional tissue section has to be done (original magnification, ×600).

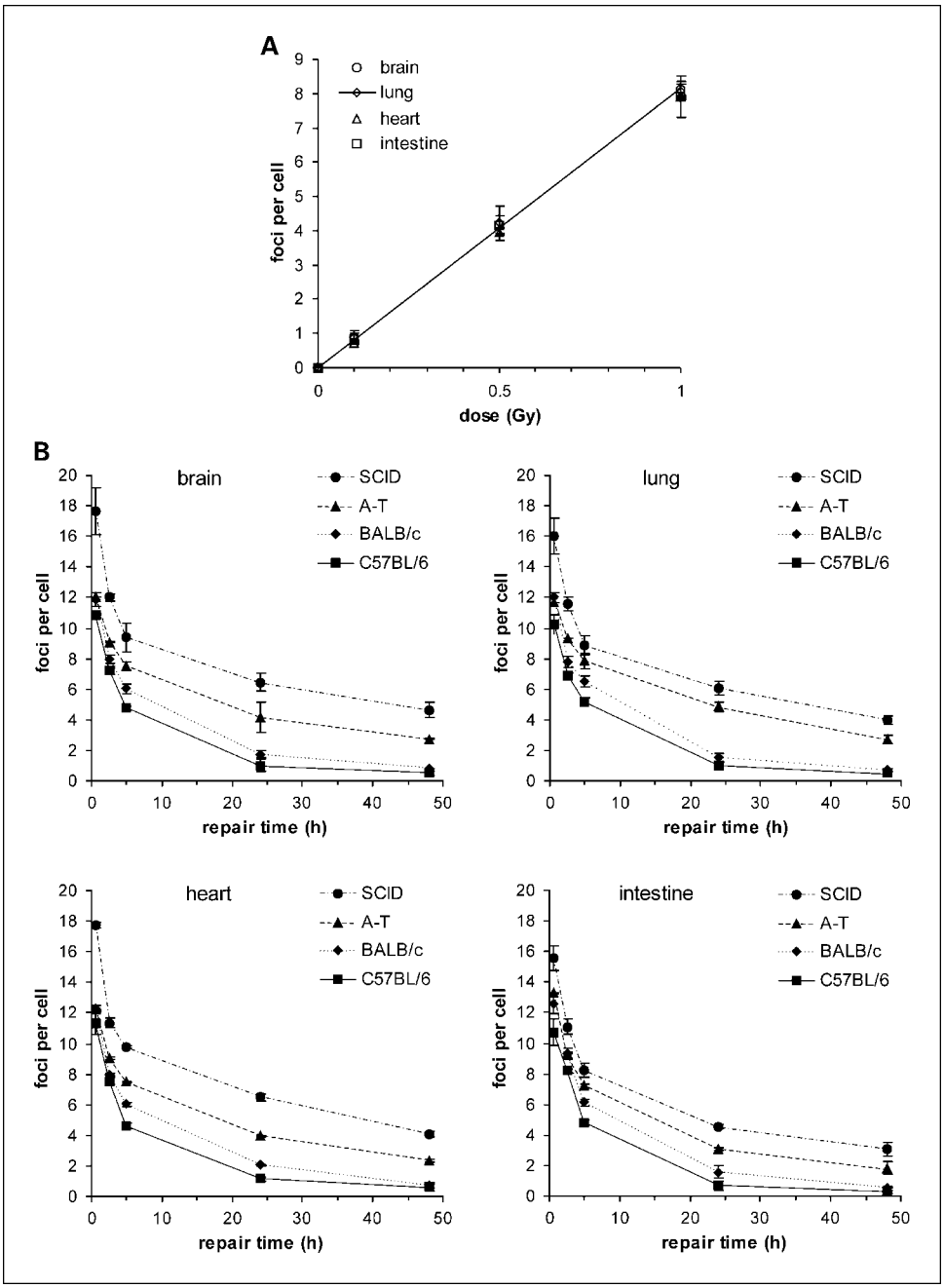

Fig. 3. *A,* DSB induction quantified by enumerating γH2AX-foci in brain, lung, heart, and small intestine at 10 min after *in vivo* irradiation of repair-proficient C57BL/6 mice. All analyzed organs revealed the same linear dose correlation from 0.1 to 1 Gy. The line is a linear fit to the data points of the lung. Points, mean from three experiments; bars, SE. *B,* DSB repair kinetics of repair-deficient (SCID, A-T, and BALB/c) and repair-proficient (C57BL/6) mouse strains evaluated by counting γH2AX-foci in brain, lung, heart, and small intestine at defined time points after *in vivo* irradiation (2 Gy). The DSB repair deficiencies of the genetically defined mouse strains can be verified in the different tissues. Points, mean from three experiments; bars, SE.

macromolecules, which is independent from the existence of DNA damage. For the quantification of DSBs, we counted the γH2AX-foci in the nuclei of the different tissues. Thus, the unspecific effect of autofluorescence had no influence on our quantitative analysis of DSB induction and repair.

In the brain, enumeration of γH2AX-foci was confined to the cerebral cortex of the midbrain, consisting of functional neuronal cells and supporting glial cells (Fig. 2A and B). In the lung, the enumeration of γH2AX-foci was confined to the bronchiolar epithelium where clearly separated nuclei allowed a reliable quantitative analysis (Fig. 2A and B). In the heart, the myocardium of ventricles consisting of striated fibers with longitudinally cut nuclei was used for γH2AX-foci analysis (Fig. 2A and B). For the analysis of DSB repair in the small intestine, the epithelial cells of the mucosal surface forming villi and crypts were analyzed for γH2AX-foci formation (Fig. 2A and B).

All images in Fig. 2B were obtained by conventional fluorescence microscopy and, thus, show optical sections providing information from only a thin focal plane. Moreover, the image acquisition of complex tissues is hampered by the fact that the various nuclei are located in different focus levels, such that the images in Fig. 2B just show variable cross-sections of nuclei varying in size and foci number. However, for enumerating γH2AX-foci per cell, the whole depth of the nuclei was scanned by focusing manually along the optical axis (*z*-direction).

DSB induction in normal tissues. Generally, the induction of DSBs is linearly dependent on the irradiation dose. However,

definite DSB induction yields of different organs may depend on tissue-specific technical demands to visualize and enumerate γH2AX-foci. Therefore, the induction of DSBs was quantified by enumerating γH2AX-foci per cell in the different tissues at 10 minutes after whole body irradiation of repair-proficient C57BL/6 mice. Ten minutes was the minimum time necessary to harvest the mice and retrieve the organs. Figure 3A shows the quantitative relationship between the number of γH2AX-foci per cell of the brain, lung, heart, and small intestine and the irradiation dose. For all analyzed organs, we observed the same linear dose correlation from 0.1 Gy (~0.8 foci per cell) to 1 Gy (~8 foci per cell).

***DSB repair in normal tissues* (in vivo).** The DSB repair kinetics of different mouse strains are shown in Fig. 3B, evaluated by counting γH2AX-foci in brain, lung, heart, and small intestine at defined time points (0.5-48 hours) after irradiation. Significantly, in all analyzed tissues, the genetically defined DSB repair defects of the different mouse strains could be clearly verified. Repair-proficient C57BL/6 mice exhibited the fastest decrease in foci number with time, and displayed only low levels of residual damage at 24 and 48 hours postirradiation. In contrast, SCID mice showed highly increased γH2AX-foci levels at all repair times ($P < 0.0001$), whereas A-T mice exhibited a lesser defect, which was most significant at later time points (≥5 hours; $P < 0.012$). Similar to our lymphocyte data (Fig. 1B), radiosensitive BALB/c mice exhibited slightly elevated foci numbers compared with C57BL/6 mice at 5 and 24 hours ($P < 0.033$; with the exception of lung 24 hours postirradiation, $P = 0.073$) but not at 48 hours postirradiation. Collectively, the DSB repair kinetics of the different mouse strains measured in various organs were nearly identical to the kinetics obtained from peripheral blood lymphocytes. Thus, data obtained in blood lymphocytes give valuable information about the DSB repair capacity of complex solid tissues of different organs.

To confirm our findings, we did an independent analysis to evaluate the DSB repair in solid tissues. Instead of counting γH2AX-foci per cell, we quantified the number of cells with ≥5 γH2AX-foci, as shown for the heart tissue in Fig. 4A. This alternative evaluation procedure provides similar results with regard to the DSB repair capacities of the different mouse strains, which support our original conclusions. In Fig. 4B, the distributions of the number of cells with n foci were included, exemplarily for the heart tissue 5 hours postirradiation. The graph shows the distributions of data points for the different mouse strains (C57BL/6, BALB/c, A-T, and SCID) and the corresponding theoretical fits of the Poisson probability distribution to these data. It is important to note that the width of the distributions does not reflect uncertainties in foci counting but is indicative of the stochastic nature of focus induction by irradiation.

To provide an independent assay of unrepaired DNA damage in solid tissues, we established the immunofluorescence staining for the p53 binding-protein 1 (53BP1), representing another highly significant marker for DSBs (36–38). 53BP1 has been shown to be recruited to sites of DSBs within several minutes after exposure to ionizing irradiation and forms irradiation-induced foci, which colocalize with γH2AX (39). In Fig. 5A, the colocalization of γH2AX and 53BP1 can clearly be shown in all analyzed tissues at 5 hours postirradiation, whereas unirradiated tissues were almost completely negative. Moreover, we counted the γH2AX- and 53BP1-foci in the double-stained tissues at 5 hours postirradiation for all mouse strains (C57BL/6, BALB/c, A-T, and SCID; Fig. 5B). The nearly identical foci counts for γH2AX and 53BP1 in a given tissue section underscore that γH2AX-foci represent reliable marker for DSBs and, thus, can be used to analyze DSB repair in normal tissues.

***DSB repair in blood lymphocytes* (ex vivo).** Finally, whole blood of BALB/c and C57BL/6 mice were irradiated *ex vivo* and DSB repair kinetics were evaluated by γH2AX-foci analysis at 0.5, 2.5, 5, and 8 hours postirradiation. Although the γH2AX-foci numbers were slightly higher compared with the *in vivo*

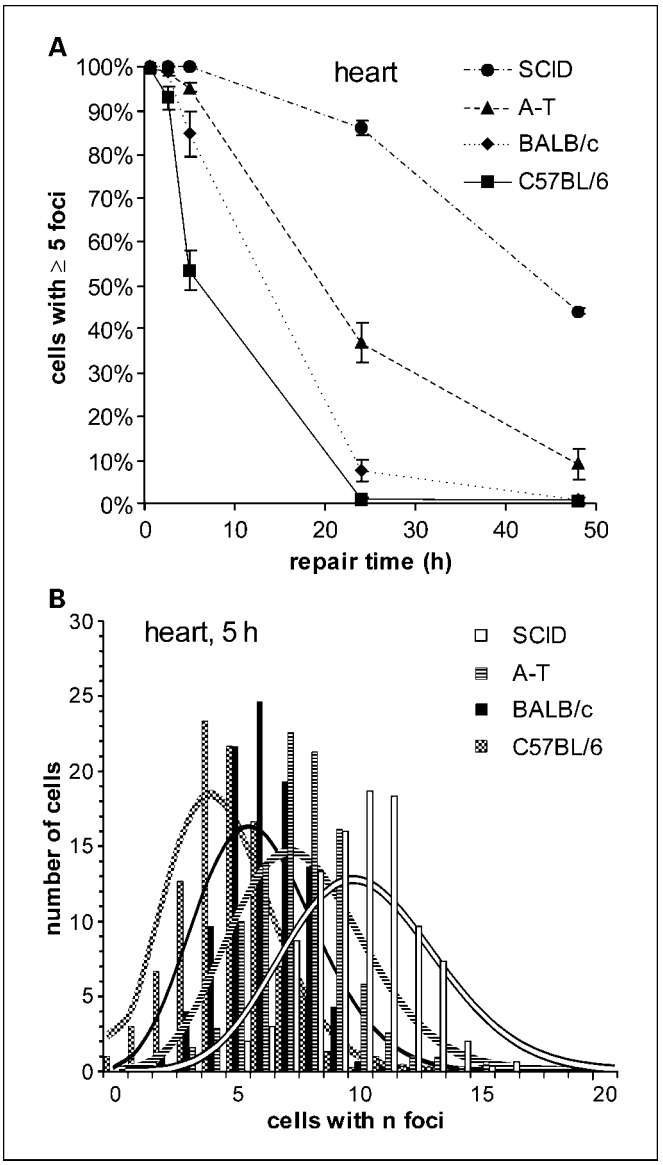

Fig. 4. *A,* quantification of the percentage of cells with ≥5 γH2AX-foci, representatively shown for the heart tissue. This alternative evaluation procedure provides similar repair kinetics and allows to verify the DSB repair deficiencies of the different mouse strains. Points, mean from three experiments; bars, SE. *B,* distribution of the number of cells with n foci, exemplarily shown for the heart tissue 5 h postirradiation. The graph shows the distributions of data points for the different mouse strains (*bar graphs*) and the theoretical fits of the Poisson probability distribution to these data (*line plots*).

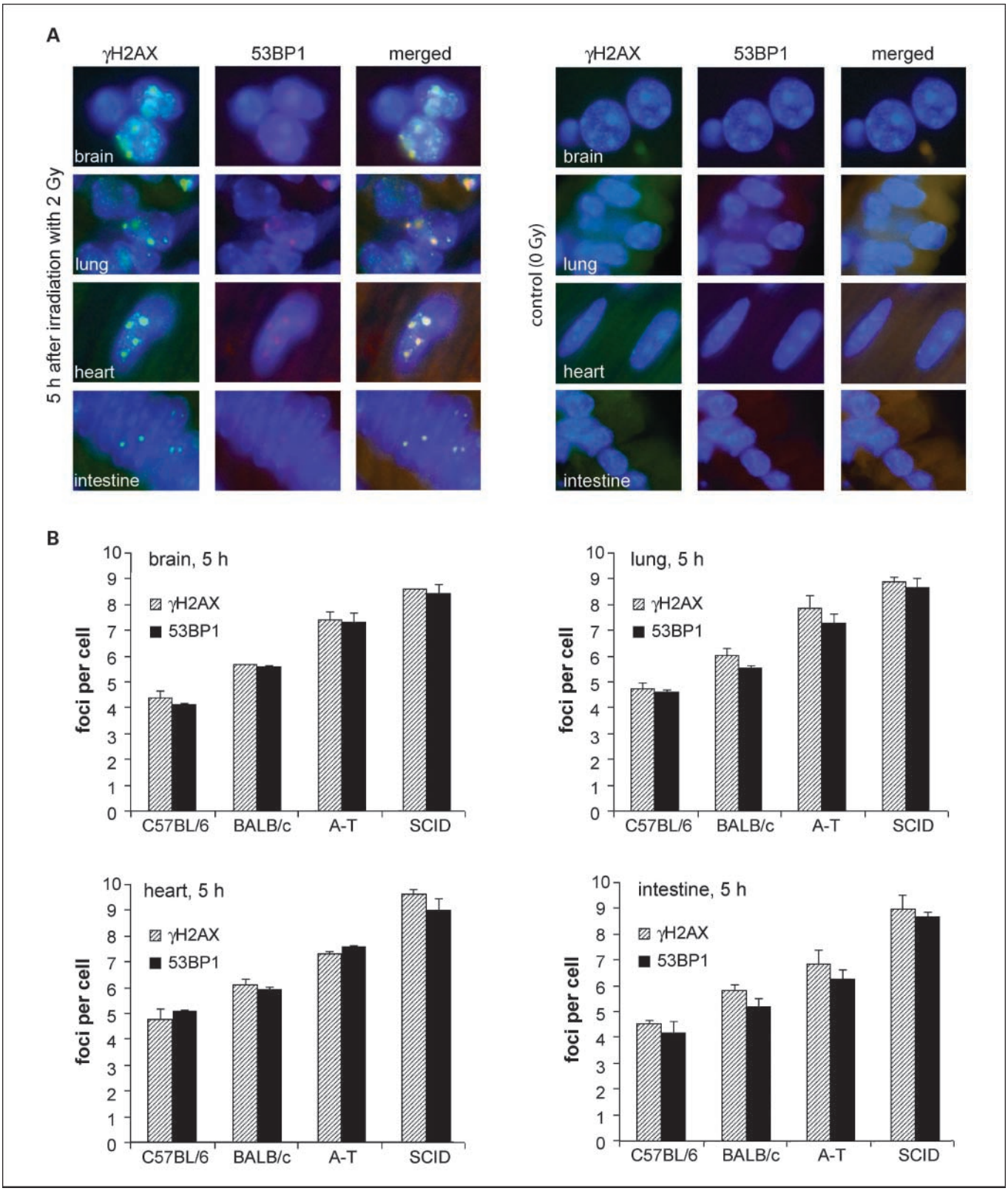

Fig. 5. *A,* immunofluorescence double-staining of γH2AX (*green*) and 53BP1 (*red*) in brain, lung, heart, and small intestine analyzed at 5 h after irradiation with 2 Gy, compared with unirradiated controls. DNA was counterstained with 4′,6-diamidino-2-phenylindole (*blue*), and images were merged to determine colocalization (*yellow*). By double labeling, the colocalization of γH2AX and 53BP1 can clearly be shown in all analyzed normal tissues at 5 h postirradiation, whereas unirradiated tissues were almost completely negative. Note that the images show just cross-sections; for enumerating γH2AX- and 53BP1-foci, a manual z-scan covering the entire nucleus in the three-dimensional tissue section has to be done (original magnification, ×1,000). *B,* analysis of γH2AX- and 53BP1-foci in brain, lung, heart, and small intestine of all mouse strains (C57BL/6, BALB/c, A-T, and SCID) obtained at 5 h after irradiation with 2 Gy. Foci analysis in the double-labeled tissues revealed nearly identical foci counts for γH2AX and 53BP1, underscoring that γH2AX-foci in normal tissues represent reliable markers for DSBs. Columns, mean from two experiments; bars, SD.

data (Fig. 1B; presumably due to a slightly slower repair process under *ex vivo* conditions), our results in Fig. 6 show that even the minor DSB repair impairment of BALB/c mice can be verified after *ex vivo* irradiation of blood samples. As blood of patients is easily accessible before radiotherapy, these results show the feasibility of the γH2AX-foci approach to screen for DSB repair deficiencies in a clinical setting.

Discussion

The present study was designed to investigate whether γH2AX-foci analysis represents a valuable tool to identify the genetically defined DSB repair capacity as determining factor for normal tissue radiosensitivity. We established the γH2AX-foci analysis to assess the induction and repair of radiation-induced DSBs in blood lymphocytes and various normal tissues of DSB repair–proficient and DSB repair–deficient mouse strains after clinically relevant irradiation doses. Analyzing the kinetics for γH2AX-foci loss allowed us to verify the different DSB repair deficiencies of the genetically defined mouse strains. Even the previously identified slight DSB repair impairment of BALB/c mice caused by a polymorphism in DNA-PKcs (24) was verified in our study by the γH2AX-foci approach in both blood lymphocytes and solid tissues, indicating that DSB repair measured in lymphocytes is valid for these different and complex organs. Based on our findings, we conclude that γH2AX-foci analysis of blood samples can give precise information about the genetically defined DSB repair status of individuals, with the potential to predict their clinical normal tissue radiosensitivity.

Validation of γH2AX-foci analysis. In a recent study by Sak et al. (40), γH2AX-foci formation in peripheral blood lymphocytes of cancer patients was analyzed after local radiotherapy for different tumor types. Although broad correlations were observed between the mean number of γH2AX-foci per lymphocyte and the integrated total body dose, several factors related to inhomogenous irradiation conditions were found to effect on the results of that clinical study (40). To circumvent these confounding factors, the animals in our experimental study received a homogenous whole-body irradiation resulting in a stochastic induction of DNA damage in all cells of the body, and thus, in all blood lymphocytes. Indeed, the distribution of the number of γH2AX-foci per cell was in agreement with the stochastic nature of radiation-induced focus formation and could be described by Poisson statistics (compare Fig. 4B).

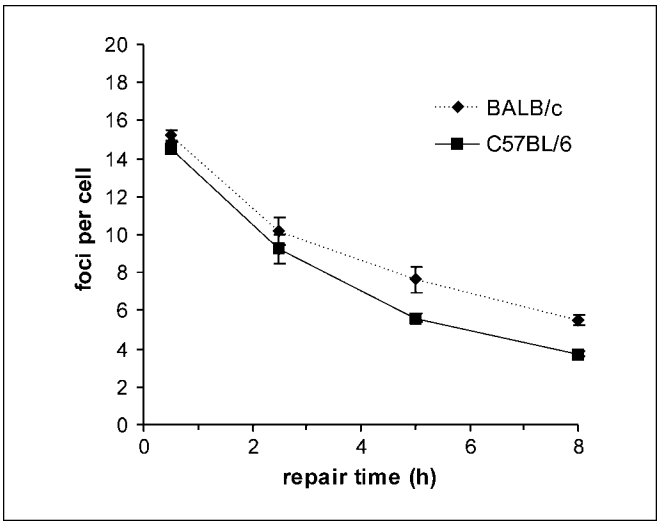

Fig. 6. γH2AX-foci analysis in blood lymphocytes of BALB/c and C57BL/6 mice after *ex vivo* irradiation (2 Gy) of blood samples. Even the DSB repair impairment of BALB/c mice can be verified by slightly increased foci numbers at 5 and 8 h postirradiation compared with repair-proficient C57BL/6 mice. Points, mean from three experiments; bars, SE.

Here, we show that radiation-induced DSBs can be monitored in various normal tissues by visualizing γH2AX-foci in formalin-fixed, paraffin-embedded tissue specimens. In contrast to other studies quantifying the total amount of γH2AX-phosphorylation in a cell or tissue area (41, 42), we counted the absolute number of γH2AX-foci formed per nucleus. Thus, even minor differences in DSB repair can be detected reliably and variations in staining intensity as well as background staining or autofluorescence have only a minor effect on quantification.

Previous *in vitro* studies showed cell cycle–dependent changes in the abundance of γH2AX in normally growing, unirradiated mammalian cell lines (43, 44). As cells progress through the active phases of the cell cycle, a gradual increase of small abundant γH2AX-foci, which do not colocalize with DNA DSB repair proteins, was observed, suggesting that γH2AX may contribute to the fidelity of the mitotic process, even in the absence of DNA damage (44). To monitor the cell cycle kinetics of the various cell populations in our analyzed organs, we did the immunohistochemical detection of Ki-67, a proliferation marker that is expressed during G_1, S, G_2, and M phases but is absent in resting G_0 cells. The Ki-67 immunohistochemistry revealed that the vast majority of cells analyzed in our study represent nonproliferating, highly differentiated cell populations with predominantly resting G_0 cells. Even in the small intestine, the proliferating precursor cells in the crypts comprise only a very small percentage of the total cell number (45). Moreover, the clear colocalization between γH2AX and 53BP1 shown in all analyzed normal tissues and their nearly identical foci counts in a given tissue section indicate that the previously described γH2AX dynamics during mitosis have not affected our experimental results (compare Fig. 5).

The exact DSB induction yields critically depend on the specific physical conditions of the irradiation (46). Whereas fibroblasts grown and irradiated on thin plastic foils (*in vitro* irradiation) reveal a DSB induction of about 20 γH2AX-foci per cell and per Gy (46), slightly lower DSB induction yields were observed in human blood lymphocytes and normal mouse tissues (47, 48). Moreover, γH2AX-foci numbers counted in murine lymphocytes (~11.5 foci/cell/Gy; compare Fig. 1B, *inset*; ~23 foci per cell after 2 Gy) were consistently lower compared with those observed in human lymphocytes (~15 foci/cell/Gy; data not shown). This can primarily be attributed to the higher DNA content of human cells compared with murine cells (3.2 Gbp compared with 2.5 Gbp; refs. 49, 50). In tissue sections, partially truncated cells were analyzed, which leads to a slight underestimation of the real foci numbers in intact cells.

Predictive testing for normal tissue radiosensitivity. In a previous clinical study, the γH2AX-foci approach was used to

assess the *in vivo* formation and loss of γH2AX-foci in lymphocytes from individuals undergoing computed tomography examination (47). In that study, a patient previously displaying severe side effects after radiotherapy exhibited levels of γH2AX-foci at various sampling times post-computed tomography that were clearly higher than those of normal individuals. γH2AX and pulsed-field gel electrophoresis analysis of fibroblasts obtained from that patient confirmed a substantial DSB repair defect. However, the precise deficiency was not identified, and it remained unclear to what extent DSB repair measured in peripheral blood lymphocytes correlates with the DSB repair of complex solid tissues.

In the present study, we analyzed γH2AX-foci kinetics in blood lymphocytes and solid tissues of mouse strains with defined genetic deficiencies in DSB repair. Our results show that DSB repair kinetics measured in peripheral blood lymphocytes are representative for all analyzed solid tissues. Thus, simple blood tests, adequate for routine clinical use, can give precise information about the genetically defined DSB repair status of individuals. As the DSB repair status is a determining factor for normal tissue responses not only after ionizing radiation, but also after treatment with other DNA-damaging agents such as certain chemotherapeutics, the γH2AX-foci approach can possibly serve as a general predictive test for clinical normal tissue toxicity in cancer treatment. Future studies have to evaluate the predictive value of this approach in the clinical setting to identify patients genetically predisposed to develop severe normal tissue toxicity.

Disclosure of Potential Conflicts of Interest

No potential conflicts of interest were disclosed.

Acknowledgments

We thank PD Dr. Gräber (Institute of Medical Biometrics, Epidemiology and Medical Informatics, Saarland University) for statistical analysis, Prof. Remberger for his continuous support and valuable comments, D. Ludwig for excellent technical assistance, J. Oelmann for major contributions in establishing the experimental procedures, and E. Gleditsch and S. Papadopolous for performing the animal experiments.

References

1. Fernet M, Hall J. Genetic biomarkers of therapeutic radiation sensitivity. DNA Repair 2004;3:1237–43.
2. Rieger KE, Hong WJ, Tusher VG, et al. Toxicity from radiation therapy associated with abnormal transcriptional responses to DNA damage. Proc Natl Acad Sci U S A 2004;101:6635–40.
3. Svensson JP, Stalpers LJ, Esveldt-van Lange RE, et al. Analysis of gene expression using gene sets discriminates cancer patients with and without late radiation toxicity. PLoS Med 2006;3:e422.
4. Bentzen SM. Preventing and reducing late side effects of radiation therapy: Radiobiology meets molecular pathology. Nat Rev Cancer 2006;6:702–13.
5. Begg AC. Can the severity of normal tissue damage after radiation therapy be predicted? PLoS Med 2006;3:e440.
6. Baumann M, Hölscher T, Begg AC. Towards genetic prediction of radiation responses: ESTRO GENEPI project. Radiother Oncol 2003;69:127–35.
7. Banath JP, MacPhail SH, Olive PL. Radiation sensitivity, H2AX phosphorylation, and kinetics of repair of DNA strand breaks in irradiated cervical cancer cell lines. Cancer Res 2004;64:7144–9.
8. Olive PL, Banath JP. Phosphorylation of histone H2AX as a measure of radiosensitivity. Int J Radiat Oncol Biol Phys 2004;58:331–5.
9. Klokov D, MacPhail SM, Banath JP, et al. Phosphorylated histone H2AX in relation to cell survival in tumor cells and xenografts exposed to single and fractionated doses of X-rays. Radiother Oncol 2006;80:223–9.
10. Taneja N, Davis M, Choy JS, et al. Histone H2AX phosphorylation as a predictor of radiosensitivity and target of radiotherapy. J Biol Chem 2004;279:2273–80.
11. O'Driscoll M, Cerosaletti KM, Girard PM, et al. DNA Ligase IV mutations identified in patients exhibiting developmental delay and immunodeficiency. Mol Cell 2001;8:1175–85.
12. Smith J, Riballo E, Kysela B, et al. Impact of DNA ligase IV on the fidelity of end joining in human cells. Nucleic Acids Res 2003;31:2157–67.
13. Girard PM, Kysela B, Härer CJ, et al. Analysis of DNA ligase IV mutations found in LIG4 syndrome patients: the impact of two linked polymorphisms. Hum Mol Genet 2004;13:2369–76.
14. Riballo E, Kühne M, Rief N, et al. A pathway of double-strand break rejoining dependent upon ATM, Artemis, and proteins locating to γH2AX foci. Mol Cell 2004;16:715–24.
15. Löbrich M, Jeggo PA. Harmonising the response to DSBs: a new string in the ATM bow. DNA Repair 2005;4:749–59.
16. Löbrich M, Jeggo PA. The impact of negligent G2/M checkpoint on genomic instability and cancer induction. Nat Rev Cancer 2007;7:861–9.
17. Rogakou EP, Pilch DR, Orr AH, et al. DNA double-strand breaks induced histone H2AX phosphorylation on Serin 139. J Biol Chem 1998;273:5858–68.
18. Rogakou EP, Boon C, Redon C, et al. Megabase chromatin domains involved in DNA double-strand breaks *in vivo*. J Cell Biol 1999;146:905–15.
19. Rothkamm K, Löbrich M. Evidence for a lack of DNA double-strand break repair in human cells exposed to very low x-ray doses. Proc Natl Acad Sci U S A 2003;100:5057–62.
20. Mahrhofer H, Bürger S, Oppitz U, et al. Radiation induced DNA damage and damage repair in human tumor and fibroblast cell lines assessed by H2AX phosphorylation. Int J Radiat Oncol Biol Phys 2006;64:573–80.
21. Araki R, Fujimori A, Hamatani K, et al. Nonsense mutation at Tyr-4046 in the DNA-dependent protein kinase catalytic subunit of severe combined immune deficiency mice. Proc Natl Acad Sci U S A 1997;94:2438–43.
22. Jeggo PA. DNA-PK: at the cross-roads of biochemistry and genetics. Mutat Res 1997;384:1–14.
23. Smith GC, Divecha N, Lakin ND, et al. DNA-dependent protein kinase and related proteins. Biochem Soc Symp 1999;64:91–104.
24. Okayasu R, Suetomi K, Yu Y, et al. A deficiency in DNA repair and DNA-PKcs expression in the radiosensitive BALB/c mouse. Cancer Res 2000;60:4342–5.
25. Mori N, Matsumoto Y, Okumoto M, et al. Variations in Prkdc encoding the catalytic subunit of DNA-dependent protein kinase (DNA-PKcs) and susceptibility to radiation-induced apoptosis and lymphomagenesis. Oncogene 2001;20:3609–19.
26. Barlow C, Hirotsune S, Paylor R, et al. Atm-deficient mice: a paradigm of ataxia telangiectasia. Cell 1996;86:159–71.
27. Lavin MF, Khanna KK. ATM: the protein encoded by the gene mutated in the radiosensitive syndrome ataxia-telangiectasia. Int J Radiat Biol 1999;75:1201–14.
28. Shiloh Y, Kastan MB. ATM: genome stability, neuronal development, and cancer cross paths. Adv Cancer Res 2001;83:209–54.
29. Ball LG, Xiao W. Molecular basis of ataxia telangiectasia and related diseases. Acta Pharmacol Sin 2005;26:897–907.
30. Kühne M, Riballo E, Rief N, et al. A double-strand break repair defect in ATM-deficient cells contributes to radiosensitivity. Cancer Res 2004;64:500–8.
31. Stiff T, O'Driscoll M, Rief N, et al. ATM and DNA-PK function redundantly to phosphorylate H2AX after exposure to ionizing radiation. Cancer Res 2004;64:2390–6.
32. Terzoudi GI, Manola KN, Pantelias GE, et al. Checkpoint abrogation in G2 compromises repair of chromosomal breaks in ataxia telangiectasia cells. Cancer Res 2005;65:11292–6.
33. Rogakou EP, Nieves-Neira W, Boon C, et al. Initiation of DNA fragmentation during apoptosis induces phosphorylation of H2AX histone at serine 139. J Biol Chem 2000;275:9390–5.
34. Lu C, Zhu F, Cho YY, et al. Cell apoptosis: requirement of H2AX in DNA ladder formation but not for the activation of caspase-3. Mol Cell 2006;23:121–32.
35. Takahashi K, Rochford CDP, Neumann H. Clearance of apoptotic neurons without inflammation by microglial triggering receptor expressed on myeloid cell-2. J Exp Med 2005;201:647–57.
36. Schultz LB, Chebab NH, Malikzay A, et al. p53 Binding Protein 1 (53BP1) is an early participant in the cellular response to DNA double-strand breaks. J Cell Biol 2000;151:1381–90.
37. Fernandez-Capetillo O, Chen HT, Celeste A, et al. DNA damage-induced G2-M checkpoint activation by histone H2AX and 53BP1. Nat Cell Biol 2002;4:993–7.
38. Wang B, Matsuoka S, Carpenter PB, et al. 53BP1, a mediator of the DNA damage checkpoint. Science 2002;298:1435–8.
39. Bekker-Jensen S, Lukas C, Melander F, et al. Dynamic assembly and sustained retention of 53BP1 at the sites of DNA damage are controlled by Mdc1/NFBD1. J Cell Biol 2005;170:201–11.
40. Sak A, Grehl S, Erichsen P, et al. γH2AX foci formation in peripheral blood lymphocytes of tumor patients after local radiotherapy to different sites of the body: dependence on the dose-distribution, irradiated site

and time from start of treatment. Int J Radiat Biol 2007;83:639–52.
41. Qvarnström OF, Simonsson M, Johansson KA, et al. DNA double strand break quantification in skin biopsies. Radiother Oncol 2004;72:311–7.
42. Olive PL, Banath JP, Sinnott LT. Phosphorylated histone H2AX in spheroids, tumors, and tissues of mice exposed to Etoposide and 3-Amino-1,2,4-Benzotriazine-1,3-Dioxide. Cancer Res 2004;64:5363–9.
43. Zhu Y, Alvarez C, Doll R, et al. Intra-S-phase checkpoint activation by direct CDK2 inhibition. Mol Cell Biol 2004;24:6268–77.
44. McManus KJ, Hendzel MJ. ATM-dependent DNA damage-independent mitotic phosphorylation of H2AX in normally growing mammalian cells. Mol Biol Cell 2005;16:5013–25.
45. Potten CS, Owen G, Booth D. Intestinal stem cells protect their genome by selective segregation of template DNA strands. J Cell Sci 2002;115:2381–8.
46. Kegel P, Riballo E, Kühne M, et al. X-irradiation of cells on glass slides has a dose doubling impact. DNA Repair 2007;6:1692–7.
47. Löbrich M, Rief N, Kühne M, et al. *In vivo* formation and repair of DNA double-strand breaks after computed tomography examinations. Proc Natl Acad Sci U S A 2005;102:8984–9.
48. Nowak E, Etienne O, Millet P, et al. Radiation-induced H2AX phosphorylation and neural precursor apoptosis in the developing brain of mice. Radiat Res 2006;165:155–64.
49. International Human Genome Sequencing Consortium: Initial sequencing and analysis of the human genome. Nature 2001;409:860–75.
50. Mouse Genome Sequencing Consortium. Initial sequencing and comparative analysis of the mouse genome. Nature 2002;420:520–62.

Clinical Cancer Research

DNA Double-Strand Break Repair of Blood Lymphocytes and Normal Tissues Analysed in a Preclinical Mouse Model: Implications for Radiosensitivity Testing

Claudia E. Rübe, Saskia Grudzenski, Martin Kühne, et al.

Clin Cancer Res 2008;14:6546-6555.